Crystal Structure and Magnetic Properties of the Compounds $Yb(Zn,Al)_{\sim 6}$ and $YbZn_{\sim 6}$

Maria L. Fornasini[a], Pietro Manfrinetti[a], Donata Mazzone[a], and Sudesh K. Dhar[b]

[a] Dipartimento di Chimica e Chim. Ind., Università di Genova, Via Dodecaneso 31, 16146 Genova, Italy
[b] CMP & MS Dept., T.I.F.R., Homi Bhabha Road, Mumbai 400 005, India

Reprint requests to Prof. M. L. Fornasini. Fax: +39 010 3628252. E-mail: cfmet@chimica.unige.it

Z. Naturforsch. **2008**, *63b,* 237 – 243; received October 8, 2007

Dedicated to Professor Evgen Ivanovich Gladyshevskii

The title compounds were synthesized and their crystal structures determined by single crystal X-ray diffraction data. Both compounds crystallize with the cubic space group $Im\bar{3}$. $Yb(Zn,Al)_{\sim 6}$: a = 14.299(4) Å, $wR(F^2) = 0.041$, with $Yb_{25.39(2)}Zn_{138.2(3)}Al_{7.7(3)}$ as the refined composition; $YbZn_{\sim 6}$: a = 14.298(4) Å, $wR(F^2) = 0.079$, with $Yb_{25.05(3)}Zn_{146.83(9)}$ as the refined composition. Their crystal structures are closely related to the YCd_6 type, with two different details: Zn/Al (or Zn) atoms in the 8*c* sites center the cubic interstices of the structure; the pentagonal dodecahedron cavities are partially filled by ytterbium atoms in the 2*a* sites, with an environment topologically similar to that found in the clathrate-I compounds. Magnetic properties of the two compounds are also reported.

Key words: Ytterbium Intermetallic Compounds, Crystal Structure, Heat Capacity, Magnetic Measurements, Resistivity

Introduction

During a study of the Yb-Zn-Al ternary system [1, 2], at the composition $Yb_{14.5}Zn_{79.5}Al_6$ a phase was identified with a body-centered cubic cell and a lattice parameter $a \sim 14.3$ Å. Several years ago one of the authors (M. L. F.) jointly with other coworkers found a phase with similar crystallographic characteristics in the Yb-Zn system [3]. At that time the compound was studied only by X-ray powder data and a relationship with the Ru_3Be_{17} structure [4] was proposed.

The aim of the present work was to determine the crystal structure and the magnetic properties of a new ternary phase and to re-examine the binary one for a possible comparison.

Experimental Section

Samples were prepared using ytterbium, zinc and aluminum with 99.9, 99.99 and 99.999 wt.-% nominal purity, respectively. Because of the high vapor pressure of both Yb and Zn, to avoid any weight losses during the reaction and melting (mainly due to the volatilization of elemental Zn), the samples had to be prepared in sealed Ta crucibles. Small pieces of Yb and Zn and turnings of Al, prepared from surface-cleaned ingots, for a total mass of about 2 g were mixed and directly pressed together into outgassed tantalum crucibles which were sealed by arc welding under a pure argon flow. The samples were melted in a high-frequency furnace by heating the crucibles up to 1100 – 1150 °C, and shaken to ensure homogenization; the crucibles were then closed under vacuum in quartz tubes and annealed in resistance furnaces. Two samples with the starting compositions $Yb_{14.5}Zn_{79.5}Al_6$ and $Yb_{14.3}Zn_{85.7}$ were annealed at 700 °C for 4 and 3 weeks, respectively. Two larger samples (4 g), having the stoichiometry determined from the structure refinements, were annealed at 720 °C for a week, and used for the physical properties characterization. No contamination of the samples by the container material was noticed, even if the reaction temperatures adopted were well above the liquidus [5].

Specimens for metallographic examination were prepared by using standard procedures and their microstructural appearance investigated by both light optical and scanning electron microscopy (LOM, SEM). The composition of the present phases was determined by electron probe microanalysis (EPMA) with an Oxford spectrometer INCA Energy 300.

Both powder and single crystal methods were utilized to perform X-ray analyses. Powder patterns were obtained by a Guinier-Stoe camera, using CuK_α radiation and pure Si as an internal standard (a = 5.4308 Å); the Guinier patterns

were indexed by comparing them with the calculated ones by means of the LAZY-PULVERIX program [6].

Single crystals, selected from samples with the starting compositions $Yb_{14.5}Zn_{79.5}Al_6$ and $Yb_{14.3}Zn_{85.7}$, were checked by Laue photographs. Single crystal intensities for both $Yb(Zn,Al)_6$ and $YbZn_6$ were collected at 293 K on a MACH3 (Bruker-Nonius) diffractometer with graphite-monochromated MoK_α radiation (λ = 0.7107 Å). For the ternary compound the lattice parameter was obtained from 25 diffractometer-measured reflections at $\theta = 25 - 30°$, while for the binary one the lattice parameter was determined from a Guinier powder pattern. An absorption correction was applied to both data sets with irregular prismatic crystal shapes, using ψ scans of two top reflections. The structure refinements were made by SHELXL-97 [7] with anisotropic displacement parameters, and the atomic coordinates were standardized by the program STRUCTURE-TIDY [8].

The magnetization of the samples was measured in a SQUID magnetometer (Quantum Design) while the electrical resistivity (1.5 – 300 K) and the heat capacity (1.5 – 40 K) were measured on home built set-ups. Typically, a DC current of 30 mA was used in the four-probe method for measuring the electrical resistance. The semi-adiabatic heat pulse method was employed to measure the heat capacity.

Structure refinements

Crystal data and selected parameters of the data collections and structure refinements are reported in Table 1. Further details of the crystal structure investigation may be obtained from Fachinformationszentrum Karlsruhe, 76344 Eggenstein-Leopoldshafen, Germany, fax: +49-7247-808-666; e-mail: crysdata@fiz-karlsruhe.de, on quoting the deposition numbers CSD-418600 ($Yb(Zn,Al)_6$), CSD-418601 ($YbZn_6$).

Preliminary X-ray data of the $Yb(Zn,Al)_6$ crystal showed a great similarity with the YCd_6 [9] structure, and its Guinier powder pattern could be easily indexed on the basis of this type. However, refinement of phases related to this structure was not straightforward owing to different types of disorder involving atoms around the cell origin.

The $YbCd_6$ structural model [10] was chosen as the starting point, but the difference Fourier synthesis immediately revealed two new positions. The first, in the cell origin, with a peak height compatible with an Yb atom, was introduced with full occupancy (Yb2), replacing the Zn atom (0.028, 0.075, 0.080) of the original model. Then a second atom in the 8*c* site (1/4, 1/4, 1/4) was added as Zn with full occupancy, because at the same time the Zn atom in the 16*f* site of the original model lowered its *x* parameter from 0.163 to 0.145 and allowed a reliable distance with the new atom to be obtained. After these insertions the $R(F)$ factor dropped to 0.058.

Table 1. Crystal structure data for the compounds $Yb(Zn/Al)_6$ and $YbZn_6$.

	$Yb(Zn,Al)_6$	$YbZn_6$
Formula	$Yb_{25.39(2)}Zn_{138.2(3)}Al_{7.7(3)}$	$Yb_{25.05(3)}Zn_{146.83(9)}$
M_r	13634.4	13936.5
Cryst. size, mm^3	$0.04 \times 0.12 \times 0.14$	$0.05 \times 0.06 \times 0.10$
Crystal system	cubic	cubic
Space group	$Im\bar{3}$ (No. 204)	$Im\bar{3}$ (No. 204)
a, Å	14.299(4)	14.298(4)
V, Å^3	2924(1)	2923(1)
Z	1	1
D_{calcd}, g cm^{-3}	7.74	7.92
μ(MoK_α), cm^{-1}	478	492
F(000), e	6021.8	6158.7
hkl range	+20, +20, +20	+20, +20, +20
$((\sin\theta)/\lambda)_{max}$, Å^{-1}	0.703	0.703
Refl. measured	2362	2363
Refl. unique	791	791
R_{int}	0.069	0.105
Param. refined	53	47
$wR(F^2)$[a] (all reflexions)	0.041	0.079
$R(F)$[a] [$F_o \geq 4\sigma(F_o)$]	0.024	0.040
GoF (F^2)[a]	0.826	0.781
Extinction coeff. x[a]	0.00016(1)	0.00012(1)
$\Delta\rho_{fin}$ (max/min), eÅ^{-3}	1.44/−1.63	3.24/−3.89

[a] $wR(F^2) = \{\Sigma[w(F_o^2 - F_c^2)^2]/\ \Sigma[w(F_o^2)^2]\}^{1/2}$; $R(F) = \Sigma||F_o| - |F_c||/\Sigma|F_o|$; GoF = $S = \{\Sigma[w(F_o^2 - F_c^2)^2]/(n-p)\}^{1/2}$; $w = 1/[\sigma^2(F_o^2) + (aP)^2]$ with $P = [2F_c^2 + \max(F_o^2, 0)]/3$; $F_c^* = k\,F_c[1 + 0.001\,x\,F_c^2\lambda^3/\sin(2\theta)]^{-1/4}$.

Table 2. Atomic coordinates and equivalent isotropic displacement parameters for $Yb_{25.39(2)}Zn_{138.2(3)}Al_{7.7(3)}$. U_{eq} is defined as $1/3(U_{11} + U_{22} + U_{33})$.

Atom	Position	x	y	z	U_{eq} (Å^2)
Yb1	24*g*	0	0.19014(3)	0.29862(3)	0.0053(1)
Yb2[a]	2*a*	0	0	0	0.0143(8)
Zn1/Al	48*h*	0.10547(6)	0.34595(6)	0.19472(6)	0.0097(3)
Zn2[b]	24*g*	0	0.066(2)	0.087(2)	0.067(9)
Zn3/Al	24*g*	0	0.23801(10)	0.08857(9)	0.0106(4)
Zn4/Al	24*g*	0	0.40535(8)	0.35031(9)	0.0071(4)
Zn5/Al	16*f*	0.14541(8)	0.14541(8)	0.14541(8)	0.0218(6)
Zn6/Al	12*e*	0.19550(13)	0	1/2	0.0081(4)
Zn7	12*d*	0.40745(14)	0	0	0.0182(4)
Zn8/Al	8*c*	1/4	1/4	1/4	0.0291(9)

[a] occ. = 0.695(8); [b] occ. = 0.076(2), isotropically refined; Zn1/Al = 0.959(6) Zn + 0.041 Al; Zn3/Al = 0.872(8) Zn + 0.128 Al; Zn4/Al = 0.960(9) Zn + 0.040 Al; Zn5/Al = 0.942(10) Zn + 0.058 Al; Zn6/Al = 0.951(10) Zn + 0.049 Al; Zn8/Al = 0.982(13) Zn + 0.018 Al.

All Zn positions were tested for possible mixed occupancies by aluminum, and a Zn/Al mixing was found for all sites, except Zn at the Wyckoff position 12*d*. After refinement with anisotropic displacement parameters, a small but significant residual in the difference Fourier synthesis was observed, with height 2.5 times the background, in a 24*g* site (0, 0.066, 0.087). This position is similar to that partially occupied by Cd and Zn, respectively, in the related $GdCd_6$ [10]

Table 3. Interatomic distances (Å) in $Yb_{25.39(2)}Zn_{138.2(3)}Al_{7.7(3)}$ with estimated standard deviations in parentheses.

Yb1–	4 Zn1/Al	3.073(1)	Yb2–	8 Zn5/Al	3.601(2)
	Zn3/Al	3.080(2)		12 Zn3/Al	3.631(2)
	2 Zn5/Al	3.087(1)			
	2 Zn1/Al	3.111(1)	Zn2–	Zn3/Al	2.46(4)
	2 Zn3/Al	3.122(1)		Zn2	2.48(7)[a]
	Zn7	3.133(1)		2 Zn5/Al	2.51(2)
	Zn4/Al	3.165(2)		2 Zn3/Al	2.68(3)
	2 Zn4/Al	3.234(1)		4 Zn2	2.69(6)[a]
	Zn6/Al	3.311(1)		Yb1	3.51(3)
	Zn2	3.51(3)[a]			
			Zn3/Al–	Zn2	2.46(4)[a]
Zn1/Al–	Zn8/Al	2.603(1)		Zn3/Al	2.533(3)
	Zn3/Al	2.638(2)		2 Zn5/Al	2.596(1)
	Zn6/Al	2.670(1)		2 Zn1/Al	2.638(2)
	Zn4/Al	2.702(1)		2 Zn2	2.68(3)[a]
	Zn4/Al	2.819(2)		Zn7	2.734(2)
	2 Zn1/Al	2.997(2)		Yb1	3.080(2)
	Zn5/Al	3.008(2)		2 Yb1	3.122(1)
	Zn1/Al	3.016(2)		Yb2	3.631(2)
	2 Yb1	3.073(1)			
	Yb1	3.111(1)	Zn5/Al–	3 Zn2	2.51(2)[a]
				Zn8/Al	2.590(2)
Zn4/Al–	Zn6/Al	2.581(2)		3 Zn3/Al	2.596(1)
	Zn6/Al	2.595(2)		3 Zn1/Al	3.008(2)
	2 Zn1/Al	2.702(1)		3 Yb1	3.087(1)
	Zn4/Al	2.707(3)		Yb2	3.601(2)
	2 Zn1/Al	2.819(2)			
	2 Zn7	2.857(2)	Zn6/Al–	2 Zn4/Al	2.581(2)
	Yb1	3.165(2)		2 Zn4/Al	2.595(2)
	2 Yb1	3.234(1)		4 Zn1/Al	2.670(1)
				2 Yb1	3.311(1)
Zn7–	Zn7	2.647(4)			
	2 Zn3/Al	2.734(2)	Zn8/Al–	2 Zn5/Al	2.590(2)
	4 Zn4/Al	2.857(2)		6 Zn1/Al	2.603(1)
	2 Yb1	3.133(1)			

[a] The number of coordinated atoms depends on the Zn2 site occupancy.

Table 4. Atomic coordinates and equivalent isotropic displacement parameters for $Yb_{25.05(3)}Zn_{146.83(9)}$. U_{eq} is defined as $1/3(U_{11}+U_{22}+U_{33})$.

Atom	Position	x	y	z	U_{eq} (Å^2)
Yb1	24g	0	0.18983(6)	0.29871(6)	0.0064(2)
Yb2[a]	2a	0	0	0	0.016(2)
Zn1	48h	0.1056(1)	0.3461(1)	0.1951(1)	0.0114(4)
Zn2[b]	24g	0	0.066(3)	0.088(3)	0.08(1)
Zn3	24g	0	0.2388(2)	0.0887(2)	0.0139(5)
Zn4	24g	0	0.4056(2)	0.3497(2)	0.0077(5)
Zn5	16f	0.1458(2)	0.1458(2)	01458(2)	0.0327(10)
Zn6	12e	0.1950(3)	0	1/2	0.0101(6)
Zn7	12d	0.4081(3)	0	0	0.0169(9)
Zn8	8c	1/4	1/4	1/4	0.042(2)

[a] occ. = 0.527(15); [b] occ. = 0.118(4), isotropically refined.

and $ScZn_6$ [11] structures. It was introduced as alternative to Yb2 in 2a. However, the site occupation undergoes a further constraint, because only three atoms instead of twelve can occur around the origin with reasonable distances. After the refinement, this site showed a filling by only 1.82(5) zinc atoms. Atomic parameters and interatomic distances of Yb(Zn,Al)$_6$ are reported in Tables 2 and 3, respectively.

The $YbZn_6$ crystal structure refinement gave similar results, but with a lower occupancy for the Yb2 site and consequently a higher number of Zn2 atoms. All other details are similar. Atomic parameters of $YbZn_6$ are given in Table 4.

Results and Discussion

Crystal structures

The structures of $YbZn_6$ and Yb(Zn,Al)$_6$ are very similar. In the ternary compound zinc and aluminum share all sites, except two which are occupied by zinc only. They can be compared with the parent structure YCd_6 [9] and with the results of recent extensive studies of the rare earth phases *RE*Cd$_6$ [10, 12] and $Sc_3Cu_yZn_{18-y}$ ($0 \leq y \leq 2.2$) [11].

All these structures are based on the same atomic arrangement with a body-centered cubic cell with $a \cong 14-15$ Å and space group $Im\bar{3}$. The interest for these phases was enhanced by the discovery of stable binary quasicrystals in the Yb-Cd and Ca-Cd systems, with compositions $YbCd_{5.7}$ and $CaCd_{5.7}$ [13], as the respective compounds $YbCd_6$ and $CaCd_6$ can be considered as approximant crystals. In these structures the main framework is practically the same, and what changes are the different details encountered on going from the cell origin along the main diagonal. As it was already pointed out [10, 11], successive shells of atoms around the origin can be observed, the most external of which gives rise to a *bcc* packing of partially interpenetrating units reproducing the whole structure. In these clusters cubic interstices are found, generally empty, but partially filled by Cd in $PrCd_6$ [10] and by Zn in $Sc_3Cu_{2.2}Zn_{16}$ [11], both crystallizing with the space group $Im\bar{3}$. Another common characteristic is the presence of a large hole around the origin, in most cases occupied by a disordered tetrahedron formed by the smaller atoms.

The two features mentioned above introduce new details for the interpretation of the $YbZn_6$ and Yb(Zn,Al)$_6$ structures. In both compounds the cubic interstices are totally filled by Zn8 and Zn8/Al, respectively in the 8c site (1/4, 1/4, 1/4). The occupation becomes total, because the atom in the 16f site, lying also on the threefold axis, approaches the origin, allowing reasonable bond lengths with the new atom to be obtained. The cube around Zn8 or Zn8/Al is prac-

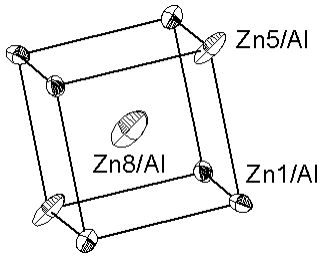

Fig. 1. Atoms surrounding Zn8/Al and forming a regular cube in the $Yb(Zn,Al)_6$ structure. All atoms are represented by their displacement ellipsoids.

tically ideal, having edge lengths of 2.99 – 3.00 and 3.00 – 3.01 Å, and angles in the ranges 89.5 – 90.8° and 89.7 – 90.5°, respectively. In Fig. 1 the Zn8/Al atom and its neighbors are represented with their displacement ellipsoids. We can note a pronounced anisotropy of the central atom and of the two Zn5/Al atoms, with elongations in the threefold axis direction. The behavior is similar to what was found by Lin and Corbett for $Sc_3Cu_{2.2}Zn_{16}$ [11], even though in that case the central zinc site has an occupation factor of only 24 %.

It is interesting to note that similar cubic interstices are filled in an ordered manner in two other related cubic compounds, Ce_6Cd_{37} described in $Pn\bar{3}$ with a similar lattice parameter [14] and Eu_4Cd_{25} with space group $Fd\bar{3}$ and a doubled lattice parameter [15]. In both compounds the cubic voids are no more equivalent, so that 1/2 and 3/4, respectively, of the voids become large enough to host cadmium atoms, while the others are contracted and remain empty.

The other detail is the occurrence of the Yb2 atom at the origin of both structures, with an occupancy reaching 69.5 % in the $Yb(Zn,Al)_6$ phase. This Yb atom, surrounded by a pentagonal dodecahedron formed by 20 Zn or Zn/Al atoms (upper part of Fig. 2), has to be considered as an alternative to the atoms labeled Zn2 in both structures, that usually fill the void around the origin. In fact, except some compounds where the filling is more complicated [10], generally the void hosts a distorted cuboctahedron formed by atoms in a 24*g* site (0*yz*) with the *y* and *z* coordinates typically about 0.077 and 0.082 [10, 12]. However, a group of 12 atoms cannot be placed around the cell origin, because too short distances within the group would occur. A possible model suggests the void to be occupied by a disordered tetrahedron, with a site occupation factor of ~ 33 %.

In the examined compounds the *y* coordinate of these atoms decreases to 0.066, and they form a distorted icosahedron instead, as shown in the lower part of Fig. 2. Now the atoms are grouped closer to the origin, and four atoms can no more coexist in the form of a tetrahedron, because any pair of atoms would have an unrealistic distance of less than 2 Å. Therefore, only a triangle of Zn2 atoms, as an alternative to the Yb2 atom, can fill the cavity in a disordered way. Each cavity can host an equilateral triangle with 8 different orientations or an isosceles triangle with 12 different orientations. The replacement of a rare earth atom by triangles of aluminum atoms has been observed in the structure of the $RE_4Pt_9Al_{24}$ compounds [16] and in the $Ho_2Rh_3Al_9$ and $Er_2Ir_3Al_9$ structures [17]. Other examples occur for the $Eu_{1-x}Ga_{2+3x}$ ($x = 0.08$) [18] and $Eu_{3-x}Ga_{8+3x}$ ($x = 0.12$) [19] structures, where a fraction of the Eu atoms is substituted by triangular Ga_3 groups.

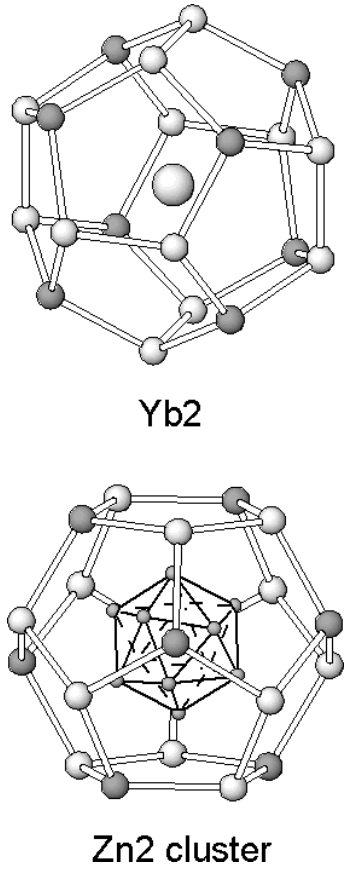

Fig. 2. Upper part: pentagonal dodecahedron formed by Zn3/Al (open circles) and Zn5/Al (full circles) around Yb2 in $Yb(Zn,Al)_6$. Lower part: the same cage viewed along the [111] direction, now containing the distorted Zn2 icosahedron. Only three out of the twelve Zn2 atoms can coexist (see text).

The occupation of the 2*a* site by the Yb2 atom in the title compounds is the main novelty, never observed before in any related structure of this family. The Yb2 atom enclosed in a pentagonal dodecahedron is reminiscent of the alkali or alkaline earth element in the 2*a* site of the cubic space group $Pm\bar{3}n$, as it appears in sev-

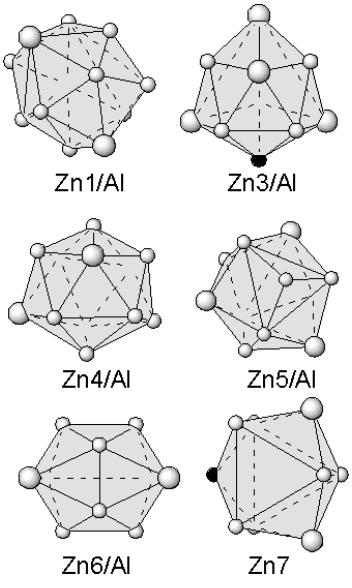

Fig. 3. Other coordination polyhedra in $Yb(Zn,Al)_6$. Large open circles: Yb; small open circles: Zn/Al; small full circles: Zn.

eral isotypic clathrate-I compounds. We can choose for comparison the β-$Ba_8Ga_{16}Sn_{30}$ structure [20] which has a ratio between Ba and Ga/Sn radii similar to the ratio between the Yb and Zn (or Zn/Al) radii. It is easy to see that both dodecahedral cages centered by Ba1 and Yb2, respectively, are practically identical, having the same topology, and the Ba1 or Yb2 atoms always coordinated by $8 + 12$ majority atoms.

Concerning the coordination of the other atoms, Yb1 is surrounded by a pentagonal prism capped on all faces. The Zn2 atom, centering one of the pentagonal faces, is present only when the origin is not occupied by Yb2. The coordination polyhedra around the other atoms in $Yb(Zn,Al)_6$ are drawn in Fig. 3. For Zn3/Al and Zn5/Al the Yb2 atom is chosen to complete the coordination, instead of an alternative Zn2 atom. The polyhedra generally have recognizable but distorted shapes. A bicapped pentagonal prism (CN12) surrounds the Zn1/Al atom, while an icosahedron is discernible around the Zn4/Al atom. Trigonal prisms formed by the majority atoms are found for both Zn5/Al and Zn7 atoms, capped on all faces (CN11) or on the lateral faces only (CN9), respectively. The Zn6/Al polyhedron (CN10) is similar to that present in several intermetallic compounds, for instance around Mn in $MnAl_6$ and around one of two Si atoms in W_5Si_3 [21]. It is formed by two quadrangular and twelve triangular faces and is called a bicapped dodecahedron [22], a decatetrahedron [23] or a sphenocorona [24].

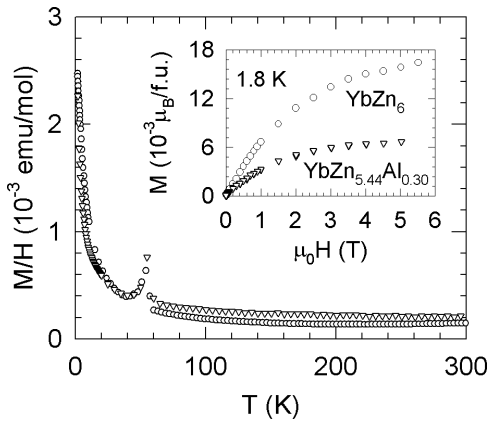

Fig. 4. Thermal variation of the magnetization M/H of $YbZn_6$ and $YbZn_{5.44}Al_{0.30}$ in an applied field of 0.3 Tesla. The inset shows the field dependence of magnetization at 1.8 K up to 5 Tesla.

Magnetic properties

Fig. 4 shows the variation of magnetization with temperature in an applied field of 3 kOe for $YbZn_6$ and $YbZn_{5.44}Al_{0.30}$. At 300 K, M/H in both compounds has a magnitude of nearly 2×10^{-4} emu mol^{-1}, implying a divalent $4f^{14}$ state of the Yb atoms. The low-temperature upturn in M/H can partly be attributed to the presence of a trace of Yb_2O_3 which is antiferromagnetic and orders magnetically near 2.3 K. Rare earth paramagnetic impurities present in Yb may also contribute to the low-temperature upturn. Concomitant with the divalent state of the Yb atoms is the low ($\sim 10^{-2}$ μ_B/f. u.) in-field magnetization at 1.8 K in the maximum applied field of 5 Tesla. The curvature in the field-dependent magnetization at 1.8 K arises due to the contribution from the trace impurity phases. There occurs a small peak in the magnetization near 60 K, which can result from frozen oxygen in the samples. Most likely the anomaly is not due to the container material as we do not see such a feature in other compounds.

The electrical resistivity of the two compounds is shown in Fig. 5. The resistivity shows metallic behavior, decreasing as the temperature is lowered. The resistivity of $YbZn_6$ and $YbZn_{5.44}Al_{0.30}$ at 300 K is 286 and 123 $\mu\Omega$ cm, respectively, varies smoothly with temperature for both compounds, and apparently does not show any anomaly around 60 K, where a peak in the magnetization is observed as described above. It may be recalled here that in the related compound

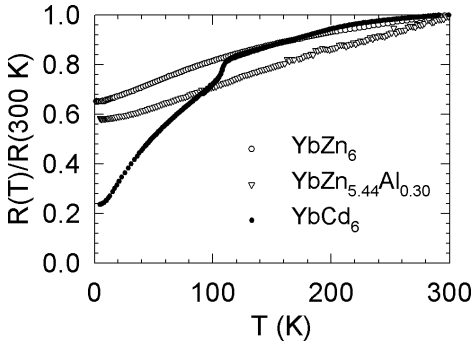

Fig. 5. The electrical resistivity of $YbZn_6$ and $YbZn_{5.44}Al_{0.30}$ plotted as $R(T)/R(300\ \mathrm{K})$. The resistivity of $YbCd_6$ [26] is also plotted for comparison.

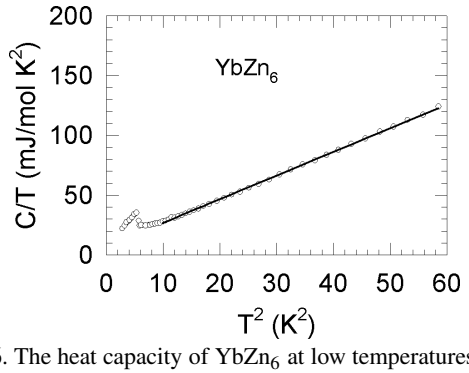

Fig. 6. The heat capacity of $YbZn_6$ at low temperatures. The solid line is a least-squares fit to the data. The peak results from a Yb_2O_3 impurity; for details see text.

$YbCd_6$, in which the Yb atoms are divalent, a disorder-to-order transition takes place at 110 K, evidenced clearly by a change of the electron diffraction pattern across the transition [25, 26]. The transition is interpreted as a low-temperature ordering of the tetrahedral Cd_4 unit inside the icosahedral cluster, described in terms of the B2 structure (changing the space group to $Pn\bar{3}$) and the B32 structure (changing the space group to $Fd\bar{3}m$ upon doubling the unit cell parameter) [25]. A signature of the transition at 110 K in $YbCd_6$ is also clearly reflected in the resistivity and heat capacity data [25, 26]. In Fig. 5 we have plotted the resistivity data for $YbCd_6$, previously published by us in ref. [26]. An anomaly at 110 K is clearly visible. Above 110 K, the temperature dependence of the resistivity of $YbCd_6$ is similar to that of $YbZn_6$ and $YbZn_{5.44}Al_{0.30}$. The susceptibility of $YbCd_6$ does not show any discernible anomaly around 110 K [26].

Finally, the heat capacity C of $YbZn_6$ is shown in Fig. 6 as a plot C/T *versus* T^2. A minor peak in the data near 2.3 K is due to the magnetic ordering of a trace amount of Yb_2O_3 present in the sample. The solid line is a least-squares fit of the expression $C/T = \gamma + \beta T^2$, where γ and β represent the electronic and lattice contributions to the heat capacity. We find $\gamma =$ 7.2 mJ mol^{-1} K^{-2} ($\sim$ 1 mJ (g atom)$^{-1}$ K^{-2}) which is a typical value for a Pauli paramagnetic metal. A value of 190.2 K is obtained for the Debye temperature, θ_D, from the fitted value of β, using the relationship $\theta_D = (1943600\,\beta^{-1})^{1/3}$ where β is in the units of mJ (g atom)$^{-1}$ K^{-4}. While the Debye temperatures of $YbZn_6$ and $YbCd_6$ are not appreciably different, 190 and 144 K, respectively, the electronic specific heat coefficient γ of $YbCd_6$ (51 mJ mol^{-1} K^{-2}) is considerably larger [26]. Presumably the difference arises due to the phase transition in $YbCd_6$.

[1] M. L. Fornasini, P. Manfrinetti, D. Mazzone, *J. Solid State Chem.* **2006**, *179*, 2012 – 2019.
[2] M. L. Fornasini, P. Manfrinetti, D. Mazzone, *Intermetallics* **2007**, *15*, 856 – 861.
[3] G. Bruzzone, M. L. Fornasini, F. Merlo, *J. Less-Common Met.* **1970**, *22*, 253 – 264.
[4] D. E. Sands, Q. C. Johnson, O. H. Krikorian, K. L. Kromholtz, *Acta Crystallogr.* **1962**, *15*, 1191 – 1195.
[5] J. T. Mason, P. Chiotti, *Trans. AIME* **1968**, *242*, 1167 – 1171.
[6] K. Yvon, W. Jeitschko, E. Parthé, *J. Appl. Crystallogr.* **1977**, *10*, 73 – 74.
[7] G. M. Sheldrick, SHELXL-97, Program for the Refinement of Crystal Structures, University of Göttingen, Göttingen (Germany) **1997**.
[8] L. M. Gelato, E. Parthé, *J. Appl. Crystallogr.* **1987**, *20*, 139 – 143.
[9] A. C. Larson, D. T. Cromer, *Acta Crystallogr.* **1971**, *B27*, 1875 – 1879.
[10] C. P. Gómez, S. Lidin, *Phys. Rev.* **2003**, *B68*, 024203 – 1/9.
[11] Q. Lin, J. D. Corbett, *Inorg. Chem.* **2004**, *43*, 1912 – 1919.
[12] S. Y. Piao, C. P. Gómez, S. Lidin, *Z. Naturforsch.* **2006**, *61b*, 644 – 649.
[13] J. Q. Guo, E. Abe, A. P. Tsai, *Phys. Rev.* **2000**, *B62*, R14605–R14608.
[14] M. Armbrüster, S. Lidin, *J. Alloys Compd.* **2000**, *307*, 141 – 148.
[15] C. P. Gómez, S. Lidin, *Chem. Eur. J.* **2004**, *10*, 3279 – 3285.

[16] V. M. T. Thiede, B. Fehrmann, W. Jeitschko, *Z. Anorg. Allg. Chem*. **1999**, *625*, 1417 – 1425.
[17] J. Niermann, B. Fehrmann, M. W. Wolff, W. Jeitschko, *J. Solid State Chem*. **2004**, *177*, 2600 – 2609.
[18] O. Sichevich, R. Ramlau, R. Giedigkeit, M. Schmidt, R. Niewa, Yu. Grin, *Abstracts 13th Int. Conf. Solid Compounds of Transition Elements*, Stresa (Italy) **2000**, pp. O – 13.
[19] O. Sichevych, Yu. Prots, Yu. Grin, *Z. Kristallogr. NCS* **2006**, *221*, 265 – 266.
[20] H. G. von Schnering, W. Carrillo-Cabrera, R. Kröner, E.-M. Peters, K. Peters, R. Nesper, *Z. Kristallogr. NCS* **1998**, *213*, 679.
[21] P. I. Kripyakevich, *Structure types of intermetallic compounds*, Nauka, Moskow, **1977**, pp.103 and 123 (in Russ.).
[22] G. A. Bandurkin, B. F. Dzhurinskii, *Zh. Strukt. Khim*. **1973**, *14*, 306 – 312.
[23] B. E. Robertson, *Inorg. Chem*. **1977**, *16*, 2735 – 2742.
[24] L. A. Aslanov, V. T. Markov, *Acta Crystallogr*. **1989**, *A45*, 661 – 671.
[25] R. Tamura. Y. Murao, S. Takeuchi, M. Ichihara, M. Isobe, Y. Ueda, *Jpn. J. Appl. Phys*. **2002**, *41*, L524 – L526.
[26] S. K. Dhar, A. Palenzona, P. Manfrinetti, S. M. Pattalwar, *J. Phys.: Condens. Matter* **2002**, *14*, 517 – 522.